Journal of Energy and Power Engineering 17 (2024) 35-45
doi: 10.17265/1934-8975/2024.02.001

Comprehensive Molten Salt Storage Shell and Support Design and Analysis III: A Complete 700 °C Thermal-Structural Interaction Design Using Theoretical Analysis of an 80 Foot Diameter and 46 Foot High MS Storage Shell Including Structural, Conductive and Convective Thermal Stress Analysis

Nathan Loyd and Samaan Ladkany
Howard Hughes College of Engineering, University This of Nevada, Las Vegas, NV 89154, USA

Abstract: This paper discusses the structural design of a futuristic 700 ℃ MS (Molten salt) Storage Shell, which considers many elements in providing an adequate and comprehensive design. In designing the structural carbon steel for the tank, temperature is an important consideration because steel has a yield strength at 700 ℃, that is 33% of its nominal yield, while the Young's Modulus at 700 °C is 50% of its nominal Young's Modulus. At this temperature, thermal stresses can yield or tear the structural steel unless free expansion of the structure is allowed. This is accomplished with sand layers below each layer of steel and by including a small gap behind the side carbon steel layer. A roof shell design for the tank is also presented in this paper, comparing various roof shell types and their designs. All designs include thermal insulation and an inner stainless steel corrosion layer to protect the structural and thermal insulation elements of the tank from the MS.

Key words: MS, storage tank design, solar energy, shell theory, steel structural design.

1. Introduction

This paper is a follow-up to our previous three papers, "Molten Salt History, Types, Thermodynamic and Physical Properties, and Cost" (2018), "565 ℃ Molten Salt Solar Energy Storage Design, Corrosion, and Insulation" (2018) and "Worldwide Molten Salt Technology Developments in Energy Production and Storage" (2018), all in the *Journal of Energy and Power Engineering*. This paper is the third paper in a four-paper follow-up series in MS (Molten salt) solar energy storage that give a complete and comprehensive analysis and design of the storage shells [1-3].

Corresponding author: Samaan Ladkany, PhD, professor, research fields: civil structural engineering, shells structures, steel structures.

1.1 Design Process for the 700°C MS Storage Shell

This paper discusses the structural design of a 700 ℃ MS Storage Shell, which considers many elements in providing an adequate and comprehensive design. When designing the use of the structural carbon steel, temperature is an important consideration because steel has a yield strength that is 33% of its nominal yield at 700 °C. Also, the Young's Modulus at 700 ℃ is 50% of its nominal Young's Modulus [4]. At this temperature, thermal stresses can be introduced to the structural steel unless free expansion of the structure is allowed. This is accomplished with sand layers below each layer of steel and by including a small gap behind

the side carbon steel layer. To meet the energy needs, two hot tanks need to be used. An axisymmetric FEA (finite element analysis) using COMSOL of the stresses in the 700 ℃ Cylindrical MS Storage Shell will be presented in another paper [5].

1.2 Corrosion Design Considerations

When designing the 700 ℃ MS Storage Shell, an important design consideration is corrosion protection, which at this temperatures use stainless steel. This is because other alloys such as Inconels exceed their structural capabilities at this temperature. There is some promise with Inconel 718 because it has a yield strength of 120 ksi at 1,200 ℉ [3, 6]. However, it was precluded from use in this design due to the lack of corrosion resistance data on Inconel 718 [5].

Under the conventional 565 ℃ MS Storage Shell, it was determined that 0.06 inches (1.52 mm) is needed to provide 30 years of protection, while 0.10 inches (2.54 mm) is needed to provide 50 years of protection [7]. However, this configuration uses solar salt as a MS while the 700 ℃ MS Storage Shell intends to use SS700 (SaltStream700) since it is designed to stay stable at 700 ℃, which has limited corrosion data. Given that, another important consideration for designing the corrosion layer is that it is able to support its own weight against buckling. With all of this information, 0.25 inches (6.35 mm) will be used as the design thickness of stainless steel as it provides a factor of safety to the corrosion design [5].

1.3 Requirements for the Prestressed Concrete Foundations

Based on prior thermal analyses that have been performed on the 700 ℃ MS Storage Shell, it is expected that the 50 inch (1.270 m) thick prestressed concrete foundation will experience higher temperatures than initially calculated. The initial thermal insulation design anticipated that the maximum temperature of the slab would be 90 ℃, but the FEA determined that the slab will be approximately 500 ℃ instead. As such, the prestressed slab is being designed with refractive concrete mixture that can handle temperatures above 400 ℃ [5, 8-10].

2. Full Design of the 700 ℃ Cylindrical MS Storage Shell

In designing the 700 ℃ Steel MS Cylindrical Shell, it should be noted that there is a layer of insulating firebrick that is in between the 316 Stainless Steel inner corrosion layer and the A588 Carbon Steel structural layer. The stainless steel will have 0.25 inches (6.35 mm) for corrosion resistance during the expected 50 year lifespan. For the design presented here, the side firebrick thickness is 10 inches (254 mm), which was determined with a heat transfer analysis. As with previous design concepts, the height of salt is 42 feet (12.802 m). However, with the tank operating at 700 ℃, the tank will use SS700, which has a unit weight of 126.7 pounds pcf (per cubic foot) at 700 ℃, instead of the conventional solar salt used at 565 ℃, which has a unit weight of 118.6 pcf at 565 ℃. The MS storage tank and the supporting layer of sand will sit on top of a 120 foot (36.576 m) diameter prestressed concrete slab, which is 50 inches thick (1.27 m). As discussed in detail later in this paper, the concrete used will be high temperature well concrete instead of conventional Portland cement. Lastly, the elliptical roof design is presented in this paper as well [5].

2.1 Bending Design of the 700°C Cylindrical MS Storage Shell

Shell theory analysis was used to design the carbon steel shell wall. This analysis determined that the axial bending dissipates 10 feet (3.048 m) above ground in the steel shell wall. The resulting bending in the steel shell wall is shown in Fig. 1. At the bottom of the shell wall, the maximum positive axial bending moment is 2.962 kip-foot/foot (13.18 kN-m/m). At a height of 2.89 feet (882 mm) above the ground, the maximum negative moment is 644.7 pound-foot/foot (2.868 kN-m/m). The resulting circumferential moments are equal to the axial moments times the

Poisson's ratio of the steel, which is 0.3. As for the circumferential force, the maximum force occurs at the bottom of the shell wall, which is 194.5 klf (kips per linear foot), or 2,838 kN/m [5].

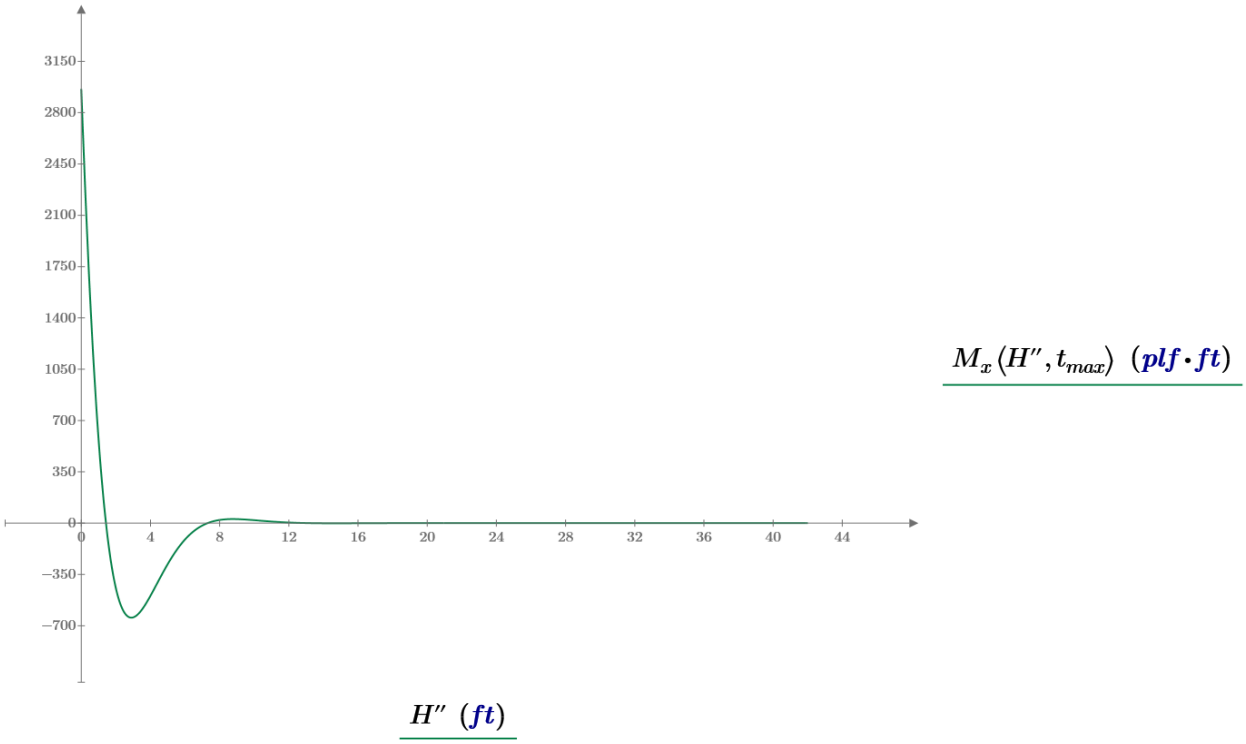

Fig. 1 Steel cylindrical shell wall M_x bending moment of the 700 ℃ Steel MS Cylindrical Shell [5].

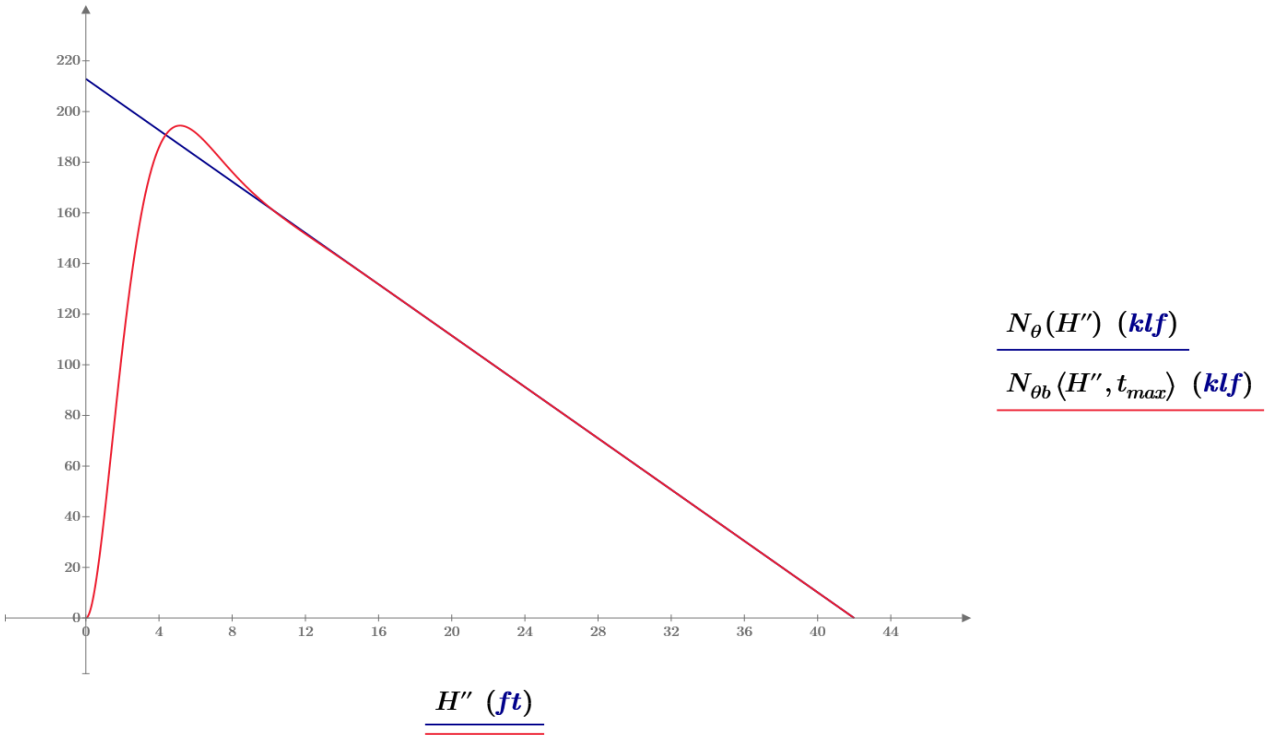

Fig. 2 Steel cylindrical shell wall N_θ forces of the 700 ℃ Steel MS Cylindrical Shell [5].
The red curve is based on Bending Theory while the blue curve is based on Shell Theory.

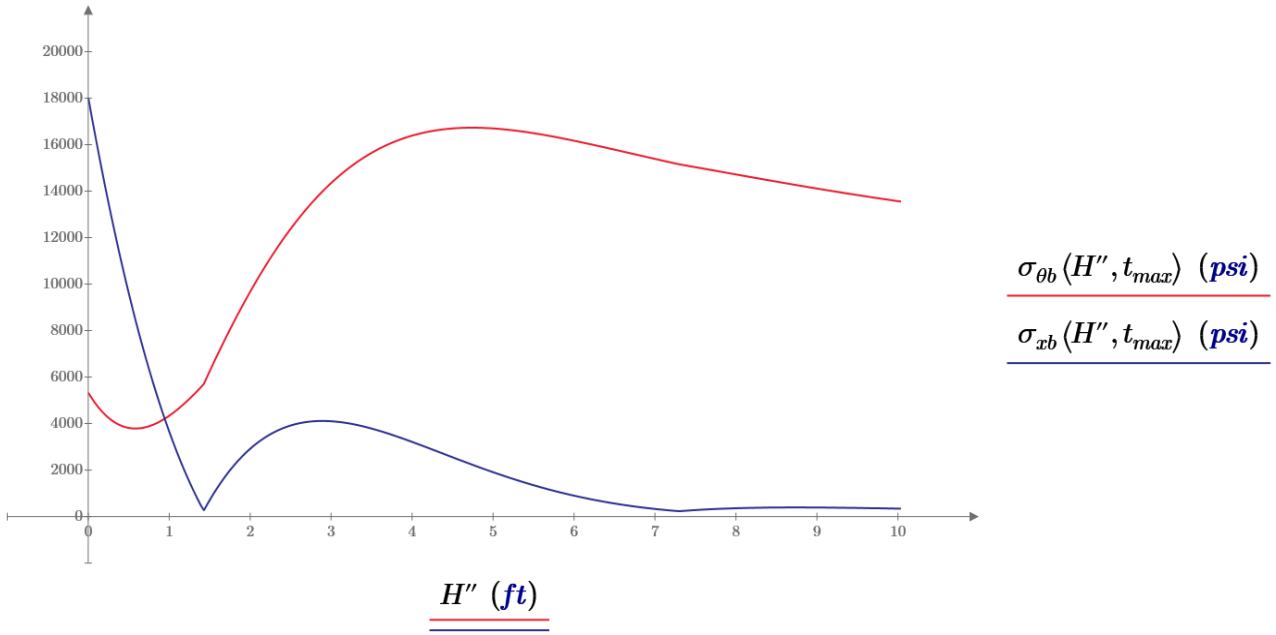

Fig. 3 Stresses at the bottom of the steel shell wall of the 700 ℃ Steel MS Cylindrical Shell [5].
The red curve is the circumferential stress and the blue curve is the axial stress.

The tensile membrane forces for the steel shell wall are shown in Fig. 2 for the steel shell wall. Shown in Fig. 3 are the circumferential and axial stresses. The maximum axial compression in the shell wall is denoted by N_x, which is equal to the total dead weight of the shell and roof shell, plus the total live load, which is the total weight (W), divided by the circumference of the shell. Buckling in the shell wall is checked by calculating the critical buckling stress (σ_{cr}). Eqs. (1)-(11) are used to perform the bending designs for the cylindrical shell [5, 11, 12]:

$$p = \gamma z \tag{1}$$

$$N_\theta = pr \tag{2}$$

$$D = \frac{Et}{12(1-\nu)} \tag{3}$$

$$\beta = \sqrt{\frac{\sqrt{1-\nu^2}}{rt}} \tag{4}$$

$$C_1 = \frac{\gamma h r^2}{Et} \tag{5}$$

$$C_2 = \frac{\gamma r^2}{Et}\left(h - \frac{1}{\beta}\right) \tag{6}$$

$$w = e^{-\beta x}(C_1 \cos\beta x + C_2 \sin\beta x) + \frac{\gamma(h-x)r^2}{Et} \tag{7}$$

$$M_x = D\frac{d^2w}{dx^2} \tag{8}$$

$$M_\theta = \nu M_x \tag{9}$$

$$N_x = \frac{W_x}{C} \tag{10}$$

$$\sigma_{cr} = \frac{Et}{r\sqrt{3(1-\nu)}} \tag{11}$$

Loyd [5] provides a full explanation of these design equations:

In determining the applied pressure on the shell from Eq. (1), it is the product of the salt unit weight (γ) and the depth of salt (z) at the specified point. In Eq. (2), p is the applied pressure on the wall and r is the radius of the wall. In Eqs. (3)- (11), D, β, C_1, and C_2 are coefficients, E is the Young's Modulus of the shell material, t is thickness of the shell wall, ν is the Poisson's ratio of the shell material, h is the total height of MS, w is shell wall deflection at a height of x above ground, and the second derivative of w is used to determine the moment at that point. M_x is the axial moment at a height of x above ground, W_x is the weight of the shell including dead and live loads on its top at level above x [11, 12].

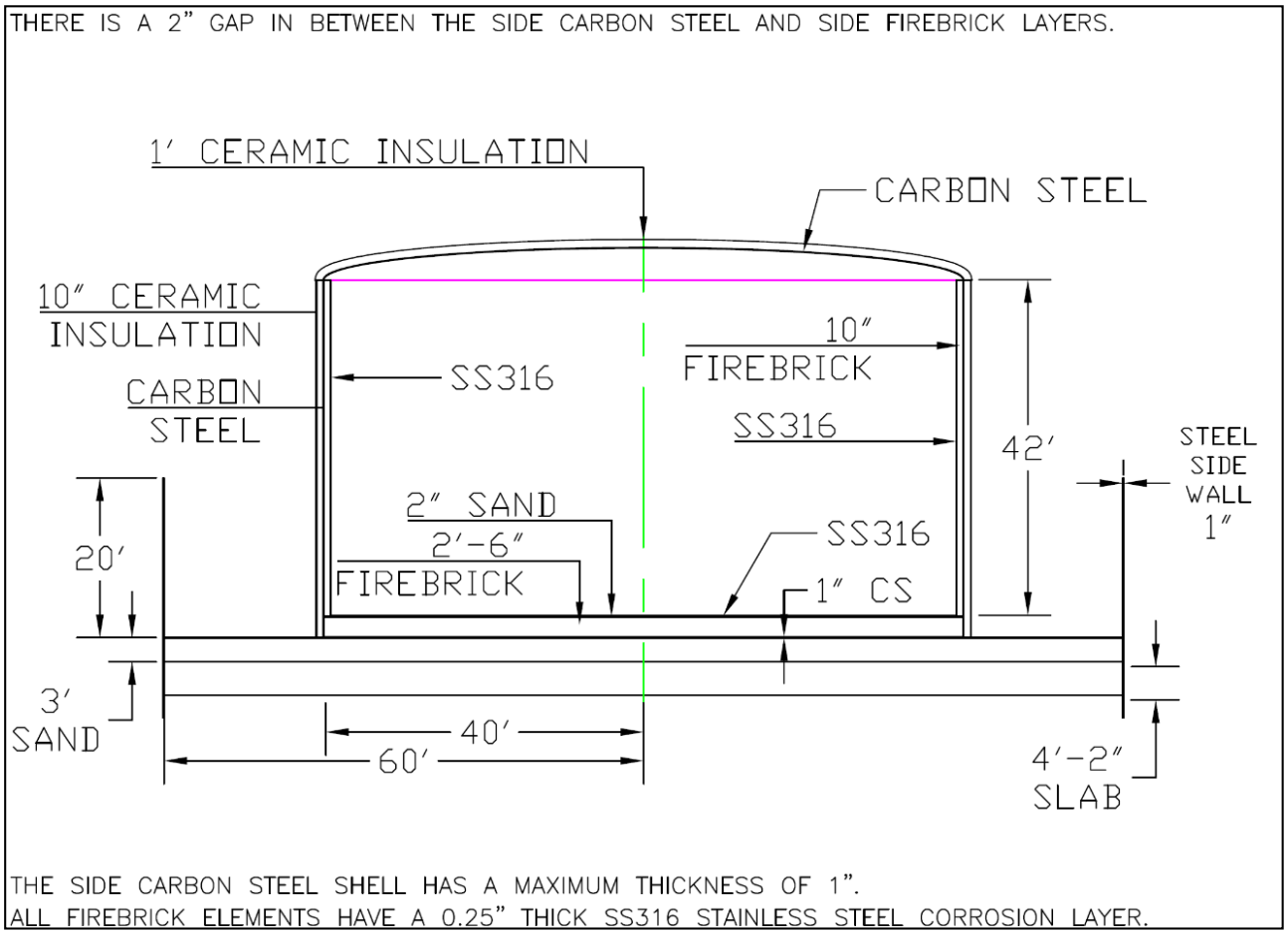

Fig. 4 700 ℃ Steel MS Cylindrical Model Design including alternative elliptical top dome, sand layer, 50″ posttension slab, and safety steel walls at the edge [5].

Fig. 4 shows the 700 ℃ Steel MS Cylindrical Shell, including the one-inch (25.4 mm) and four-foot (1.219 m) high elliptical roof shell. The side carbon steel shell wall thickness is variable due to the loading from the MS. For the bottom 11 feet (3.353 m) of the shell wall, the required thickness is 7/8 inches (22.2 mm). This is due to the combination of bending and axial forces. However, 1 inch (25.4 mm) is used to match the same 1 inch thickness of the carbon steel plate that is connected to the shell wall at the bottom. These two elements are connected together with a revolved L6×6×1″ angle section [5].

Once the shell wall is 11 feet above ground (3.353 m), bending dissipates in the carbon steel shell wall and as such, only needs to be designed for axial forces. The required steel thickness is 0.625 inches (15.9 mm) for a height that is between 11 and 17 feet (3.353 and 5.182 m). The required steel thickness is 0.5 inches (12.7 mm) for a height that is between 17 and 23 feet (5.182 and 7.010 m). The required steel thickness is 0.375 inches (9.5 mm) for a height that is between 23 and 30 feet (7.010 and 9.144 m). The required steel thickness is 0.25 inches (6.4 mm) for a height that is between 30 and 36 feet (9.144 and 10.973 m). The required steel thickness is 0.125 inches (3.2 mm) for a height above 36 feet (10.973 m) [5].

2.2 Thermal Structural Effects of the 700°C Cylindrical MS Storage Shell

In designing the 700 ℃ MS Storage Shell, thermal effects had to be accounted for in the design. The firebrick insulation is designed to keep the carbon steel

storage shell around 565 ℃, and as such that is assumed to be the heated temperature of the carbon steel shell. With an expected construction temperature of 20 ℃, the resulting temperature difference between these two temperatures will be the ΔT in Eq. (12). Eq. (12) is used to calculate the free thermal expansion of the steel, with α being the respective rate thermal expansion. Free thermal expansion is allowed for in the design with a three-foot (914 mm) sand layer below the bottom carbon steel layer and a two-inch (50.8 mm) sand layer below the bottom stainless steel layer. Due to the difference in thermal expansion rates between the two types of steel (12.5×10^{-6} for Carbon Steel and 16×10^{-6} for Stainless Steel), there will either be thermal stresses in the steel layers, or there will be a gap that is needed to allow for the complete thermal expansion [13]. Free thermal expansion deflection (Δ_t) is determined by Eq. (13), while Eq. (14) details the thermal stress (σ_t) that occurs when a corresponding thermal expansion (ε_t) is constrained from thermal expansion. In these equations, L is the characteristic length of the material expanding while E is the Young's Modulus of the material [5].

$$\varepsilon_t = \alpha * \Delta T \quad (12)$$

$$\Delta_t = \varepsilon_t * L \quad (13)$$

$$\sigma_t = \varepsilon_t * E \quad (14)$$

Free thermal expansion is allowed for in the design with a three-foot (914 mm) sand layer below the bottom carbon steel layer and a two-inch (50.8 mm) sand layer below the bottom stainless steel layer. However, based on the differing expansion rates of the two steels, the resulting constrained thermal stress in the stainless steel is 69.0 ksi (kips per square inch) at 700 ℃, exceed the allowable stress of 11.9 ksi at this temperature. As such, a gap must be allowed behind the carbon steel layer to allow for both the stainless steel and the firebrick insulation to expand into the carbon steel layer. With a temperature of 700 ℃ and a radius of 40 feet (12.192 m), the resulting free expansion deflection of the stainless steel is 5.222 inches (133 mm) [5].

Based on this, the resulting gap that is needed is two inches (50.8 mm) between the carbon steel and firebrick. This will result in all three layers converging when completely heated because the firebrick insulation has a smaller thermal expansion rate (6×10^{-6}) than both the steel layers [13]. The low expansion rate is why both the side and bottom layers of firebrick insulation will develop microcracking when heated and expanded. With a nine-inch (229 mm) brick, this would result in microcracks of 0.04 inches (1.0 mm) between each brick. With the stainless steel expanding faster than the carbon steel, it was also determined that the height reduction of the side stainless steel by 1.812 inches (46.0 mm) so that the stainless steel does not expand above the carbon steel layer [5].

Due to the thermal effects of the 700 ℃ Steel MS Cylindrical Shell, it is recommended that the tank be filled quickly so that the whole wall heats together, which would allow the side stainless steel layer to push the side firebrick layer into the side carbon steel layer all at once [5].

3. MS Storage Tank Roof Shell Design

Using A529 Grade 42 steel, a steel design was performed on elliptical, parabolic, and spherical shells for the 700 ℃ Cylindrical MS Storage Tank, with such roof shells shown in Fig. 5. When designing the roof shells for the 700 ℃ Cylindrical MS Storage Tank, the radius at the base of the roof shell is dependent of the firebrick insulation and as such can vary based on the expected design temperature. For the design presented here, the base radius for all roof shapes is 41 feet (12.497 m). For each roof shape, a design was performed for heights of 4 feet (1.219 m), 8 feet (2.438 meters), and 12 feet (3.658 m). The final shape chosen was the four-foot high elliptical shell roof [5].

Presented in Table 1 are the geometries of the 700 ℃ Cylindrical MS Shells. Loyd [5] details the roof design equations and how the geometry affects the design of the roof shells.

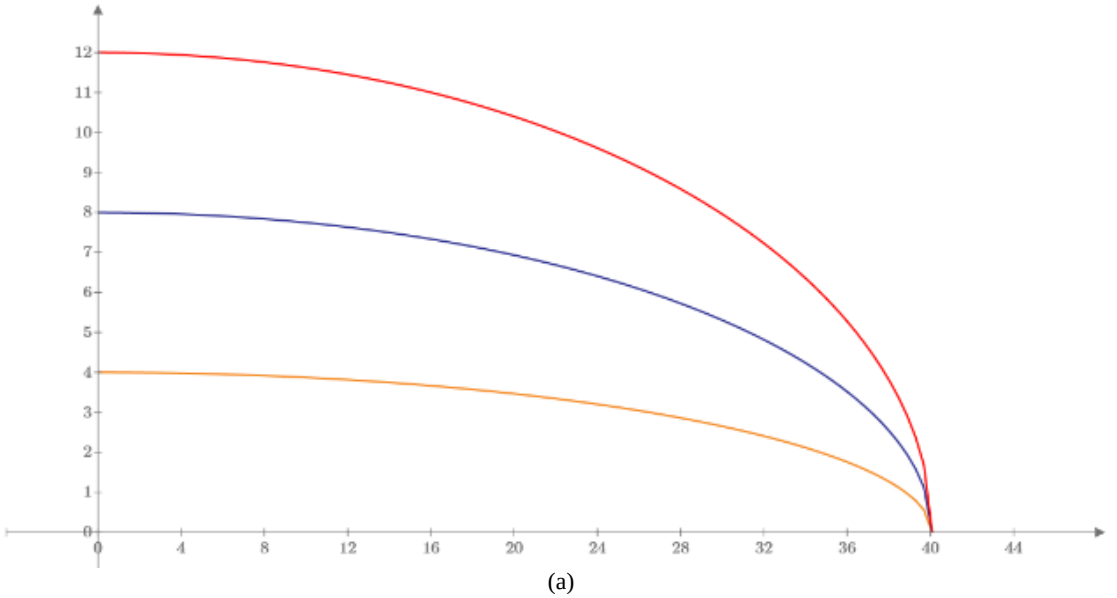

(a)

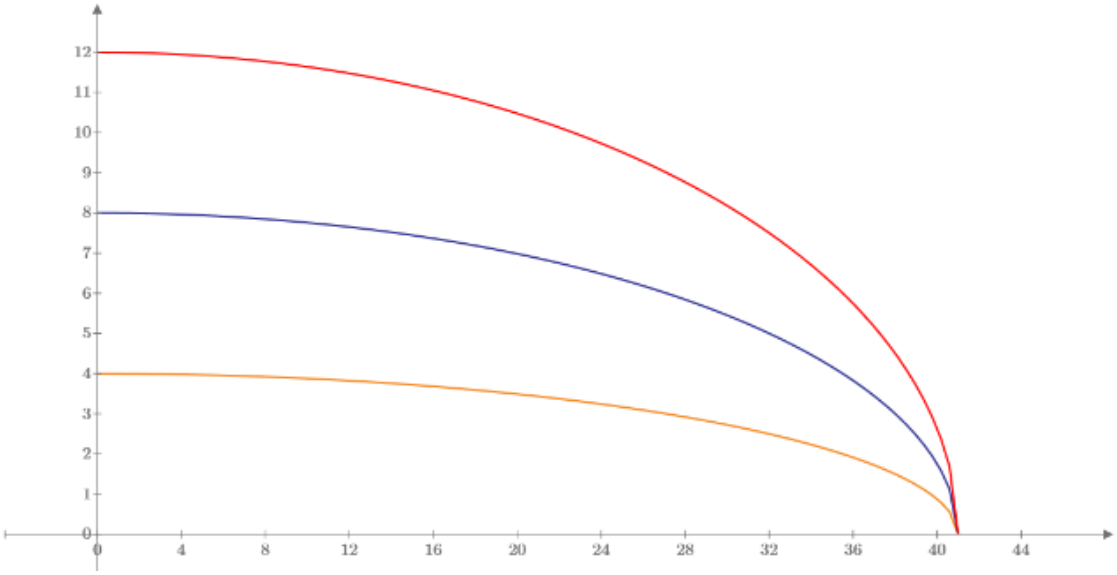

(b)

Fig. 5 Roof Shell Models for the 565 ℃ Cylindrical MS Shell (a) and the 700 ℃ Cylindrical MS Shell (b) [5].

The 12′ high roofs are in Red, 8′ high roofs in Blue, and 4′ high roofs in Blue.

The x-axes are the distance from the centerline while the y-axes are the heights of the roof shells.

Table 1 Radius of curvature of shells with a 41′ radius at the base of the shell [5].

Type of shell	Spherical shells			Parabolic shells			Elliptical shells		
Height of shell (ft)	4′	8′	12′	4′	8′	12′	4′	8′	12′
Shell R_0 at apex of shell (ft)	212.1	109.1	76.0	210.1	105.1	70.0	420.3	210.1	140.1
Shell r_1 at an angle of $\phi_r/2$ (ft)	212.1	109.1	76.0	213.1	110.7	77.9	1.1	4.2	8.8
Shell r_2 at an angle of $\phi_r/2$ (ft)	212.1	109.1	76.0	211.1	107.0	72.6	57.7	56.9	55.6
Shell r_1 at base of shell (ft)	212.1	109.1	76.0	222.2	130.0	109.0	0.4	1.6	3.5
Shell r_2 at base of shell (ft)	212.1	109.1	76.0	214.1	112.8	81.2	41.0	41.0	41.0
ϕ_r angle at base of curve (°)	11.1	22.1	32.6	11.0	21.4	30.3	90.0	90.0	90.0

In shell design, there are typically two radii of curvature that are used in determining the shell forces, r_1 which is the radial radius of curvature, and r_2 which is the circumferential radius of curvature. At the apex of any shell, r_1 and r_2 are equal to each other and referred to as R_0. In addition, r_1 and r_2 are equal to each other at any given point in a spherical shell, meaning R_0 exists at every point in the shell. The phi (ϕ_r) angle of the shell is the angular measure of the arc between the axis of revolution and the edge of the shell. Eqs. (15)-(17) detail how R_0 is calculated for a parabolic shell, elliptical shell, and spherical shell respectively [12].

$$R_0 = \frac{a^2}{2H} \tag{15}$$

$$R_0 = \frac{a^2}{H} \tag{16}$$

$$R_0 = \frac{a^2}{2H} + \frac{H}{2} \tag{17}$$

In Eqs. (15)-(17), a represents the radius of revolution of the shell at the base of the shell. In addition, H is the height of the shell above the base. Eqs. (18) and (19) detail how to calculate r_1 and r_2 for each shell, respectively [14].

$$r_1 = \frac{R_0}{(1+\gamma \sin^2\phi)^{1.5}} \tag{18}$$

$$r_2 = \frac{R_0}{(1+\gamma \sin^2\phi)^{0.5}} \tag{19}$$

In Eqs. (18) and (19), ϕ is the angle from the axis of revolution on top of the shell to any point of the shell and γ is the shape factor for the type of shell, which is 0 for a spherical shell and -1 for a parabolic shell. Eq. (20) is used to determine γ for elliptical shells [14].

$$\gamma = \frac{a^2}{H^2} - 1 \tag{20}$$

These shells were designed using shell theory to determine the thickness of each shell using various load combinations for wind and gravity loading. Shown in Eqs. (21) and (22) are the shell forces due to gravity loads, dead and live in each shell. Eq. (23) is the wind loading on each shell, it represents compressive pressure loading on the shell surface facing the wind and suction on the opposite face of the shell. Eqs. (24)-(26) are the shell forces due to wind loading in each shell.

$$N_\phi = -\int_0^{\phi_r} p r_1 r_2 \cos\phi \sin\phi \, d\phi \tag{21}$$

$$N_\theta = -p r_2 - \frac{N_\phi r_2}{r_1} \tag{22}$$

$$p_{wind} = p_w \cos\theta \sin\phi \tag{23}$$

$$N_\phi = -\frac{p_w r \cos\theta \cos\phi}{3\sin^3\phi}(2 - 3\cos\phi + \cos^3\phi) \tag{24}$$

$$N_\theta = \frac{p_w r \cos\theta}{3\sin^3\phi}(2\cos\phi - 3\sin^2\phi - 2\cos^4\phi) \tag{25}$$

$$N_{\phi\theta} = -\frac{p_w r \sin\theta}{3\sin^3\phi}(2 - 3\cos\phi + \cos^3\phi) \tag{26}$$

In Eq. (21), N_ϕ is the shell force in the radial direction in each shell due to dead and live gravity loading. In Eq. (22), N_θ is the shell force in the circumferential direction in each shell due to gravity loading. In Eq. (23), θ is the angle around the shell in the circumferential direction, with $0°$ representing where the maximum wind loading on the shell occurs. In addition, p_{wind} is the wind loading at any given point on the shell while p_w is the maximum wind pressure, which in this design is 40 pounds per square foot and equivalent to a wind speed of 125 mile/h. In Eq. (24), N_ϕ is the shell force in the radial direction in each shell due to wind loading. In Eq. (25), N_θ is the shell force in the circumferential direction in each shell due to wind loading. In Eq. (26), $N_{\phi\theta}$ is the shell force due to shear in each shell due to wind loading. In Eqs. (24)-(26), r is the largest of r_1 and r_2. For each shell, load combinations specified in ASCE-7 are used to combine the forces in the shell N_ϕ, N_θ, and $N_{\phi\theta}$ due to wind with N_ϕ, N_θ, due to dead and live loads for each shell. Shell force combinations, for N_ϕ, N_θ, and $N_{\phi\theta}$ are then divided by the usable portion of the yield strength of steel at MS temperature to determine various thicknesses for the shell designs.

In A529 Grade 42 steel, the yield stress is 42 ksi at room temperature. At 565 ℃, the design temperature of the roof shell, the yield strength is only 60% of its original yield strength, resulting in a yield strength of 25.2 ksi for the steel [4]. Shown in Table 2 are the maximum thicknesses of each shell with design including and excluding wind effects for the 700 ℃ Cylindrical MS Shells [5].

The roof shell designed examined the effects of buckling in the roof shells, which ultimately controlled the final design. Table 3 shows the required shell thicknesses based on the buckling designs, the shell thickness used in determining the final size of the ring connecting the shell to the shell, and lastly, the size of the connecting ring between the roof shell and side shell wall, for the 700 ℃ Cylindrical MS Shell. Loyd [5] details these design aspects further.

Eq. (27) shows how the thickness was calculated to satisfy buckling [11]. Based on Eq. (27), E is the Young's Modulus of the steel. The Young's Modulus of steel is typically 29,000 ksi, but at 565 ℃, the Young's Modulus is 65% of its original value, which is 18,850 ksi [4]. In addition, ν is the Poisson's ratio of the steel shell, which is 0.3. R is the larger of r_1 or r_2 at any given angle ϕ. FS is the factor of safety used in the design, which is 1.67, and p_s is the service loading on the shell at an angle ϕ. Lastly, t is the thickness of the shell needed to satisfy the given equation.

$$\frac{2Et^2}{\sqrt{3(1-\nu^2)R^2\cos\phi}} = FS * p_s(\phi) \qquad (27)$$

For the 700 ℃ Cylindrical MS Shell, the spherical shells require thicknesses of 0.33 inches, 0.16 inches, and 0.11 inches for the shells with a height of 4 feet, 8 feet, and 12 feet respectively. The parabolic shells require thicknesses of 0.35 inches, 0.17 inches, and 0.13 for the shells with a height of 4 feet, 8 feet, and 12 feet respectively. The elliptical shells require thicknesses of 0.84 inches, 0.33 inches, and 0.21 inches for the shells with a height of 4 feet, 8 feet, and 12 feet respectively. Based on these thicknesses, the spherical shells must have minimum thicknesses of 0.35 inches, 0.20 inches, and 0.15 inches for the shells with a height of 4 feet, 8 feet, and 12 feet respectively. The parabolic shells must have minimum thicknesses of 0.35 inches, 0.20 inches, and 0.15 inches for the shells with a height of 4 feet, 8 feet, and 12 feet respectively. The elliptical shells must have minimum thicknesses of 0.85 inches, 0.35 inches, and 0.25 inches for the shells with a height of 4 feet, 8 feet, and 12 feet respectively.

Eq. (28) shows the formula for determining the ring sectional area (A_r) of a supporting ring with a given Young's modulus (E_r), a calculated ring force (P_r) in the cross section, as well as a calculated roof strain (ε_r). Eq. (29) is used to calculate the ring forces for rings supporting spherical and parabolic rings, with N_ϕ

Table 2 Shell theory required thickness with a 41′ radius at the base of shell [5].

Type of shell	Spherical shells			Parabolic shells			Elliptical shells		
Height of shell (ft)	4′	8′	12′	4′	8′	12′	4′	8′	12′
Shell thickness w/o wind (in.)	0.012	0.006	0.004	0.013	0.006	0.004	0.399	0.063	0.025
Shell thickness with wind (in.)	0.025	0.013	0.009	0.025	0.015	0.012	0.403	0.066	0.027

Table 3 Buckling controlled design thickness with a 41′ radius at the base of shell [5].

Type of shell	Spherical shells			Parabolic shells			Elliptical shells		
Height of shell (ft)	4′	8′	12′	4′	8′	12′	4′	8′	12′
Required shell thickness (in.)	0.33	0.16	0.11	0.35	0.17	0.13	0.84	0.33	0.21
Minimum shell thickness (in.)	0.35	0.20	0.15	0.35	0.20	0.15	0.85	0.35	0.25
Phi angle of max buckling (°)	0.0	0.0	0.0	11.0	21.4	30.3	0.0	0.0	0.0
Ring cross sectional area (in.^{2})	252.2	159.8	154.9	238.9	127.8	88.4	6.2	17.0	32.7

being the roof shell force in the phi direction and ϕ being the phi angle of the roof at the support. Eq. (30) is used to calculate the ring forces for rings supporting elliptical shells, with $N_{\phi\theta}$ being the roof shear forces along the ring support and θ being the theta angle of the roof along the ring support. In both Eqs. (29) and (30), r is the radius of the support ring.

$$A_r = \left|\frac{P_r}{\varepsilon_r \ E_r}\right| \tag{28}$$

$$P_r = -N_\phi \ r\cos\phi \tag{29}$$

$$P_r = -r\int_0^\pi N_{\phi\theta}\sin\theta \, d\theta \tag{30}$$

For the 700 ℃ Cylindrical MS Shell, the spherical shells have ring cross sectional areas of 252.2 square inches, 159.8 square inches, and 154.9 square inches for the shells with a height of 4 feet, 8 feet, and 12 feet respectively. The parabolic shells have ring cross sectional areas of 238.9 square inches, 127.8 square inches, and 88.4 square inches for the shells with a height of 4 feet, 8 feet, and 12 feet respectively. The elliptical shells have ring cross sectional areas of 6.2 square inches, 17.0 square inches, and 32.7 square inches for the shells with a height of 4 feet, 8 feet, and 12 feet respectively. Each ring will use A588 Grade 60 steel.

4. Conclusions

After performing an exhaustive structural design for the 700 ℃ Cylindrical MS Shell, it was determined that the shell would be 80 feet high in radius, with a height of 42 feet. This shell wall includes the structural shell wall, as well as the firebrick and ceramic fiber thermal insulation. On top of the tank is the four-foot high elliptical roof shell, while the bottom of the tank includes a carbon steel plate that also has firebrick insulation as well as sand, the latter allowing for full thermal expansion for the bottom of the tank. The inside of the tank includes a ¼ inch thick SS316 stainless steel corrosion liner to protect the structural and thermal insulating elements of the tank from the MS.

Acknowledgments

Our funding for this research came from the ONR (Office of Naval Research). Further support has also come from the University of Nevada, Las Vegas, the Howard Hughes College of Engineering, and the Department of Civil and Environmental Engineering and Construction.

References

[1] Ladkany, S., Culbreth, W., and Loyd, N. 2018. “Molten Salt History, Types, Thermodynamic and Physical Properties, and Cost.” *Journal of Energy and Power Engineering* 12 (11): 507-16.

[2] Ladkany, S., Culbreth, W., and Loyd, N. 2018. “565°C Molten Salt Solar Energy Storage Design, Corrosion, and Insulation.” *Journal of Energy and Power Engineering* 12 (11): 571-32.

[3] Ladkany, S., Culbreth, W., and Loyd, N. 2018. “Worldwide Molten Salt Technology Developments in Energy Production and Storage”. *Journal of Energy and Power Engineering* 12 (11): 533-44.

[4] Salmon, C. G., Johnson, J. E., and Malhas, F. A. 2009. *Steel Structures: Design and Behavior* (5th ed.). Upper Saddle River, NJ: Pearson Prentice Hall.

[5] Loyd, N. 2020. “Alternate Novel Thermal Structure Interaction Designs of Molten Salt Shell Structures at High Temperatures Ranging from 565 ℃ to 700 ℃.” PhD thesis, University of Nevada.

[6] Special Metals. 2007. “Inconel Alloy 718 Data Sheet.” https://www.specialmetals.com/assets/smc/documents/inconel_alloy_718.pdf.

[7] Bradshaw, R. W., and Goods, S. H. 2001. “Corrosion Resistance of Stainless Steels during Thermal Cycling in Alkali Nitrate Molten Salts.” Sandia National Laboratory.

[8] Chan, Y. N., Peng, G., and Chan, J. K. W. 1996. “Comparison between High Strength Concrete and Normal Strength Concrete Subjected to High Temperature.” *Materials and Structures* 29: 616-9.

[9] Chan, Y. N., Luo, X., and Sun, W. 2000. “Compressive Strength and Pore Structure of High Performance Concrete after Exposure to High Temperature up to 800 ℃.” *Cement and Concrete Research* 30: 247-51.

[10] Liang, X., Wu, C. Q., Su, Y., Chen, Z., and Li, Z. X. 2018. “Development of Ultra-High Performance Concrete with High Fire Resistance.” *Construction and Building Materials* 179: 400-12.

[11] Timoshenko, S. 1959. *Theory of Plates and Shells*. New

York: McGraw-Hill.

[12] Urugal, A. C. 2009. *Theory of Beams, Plates, and Shells* (4th ed.). Boca Raton, FL: CRC Press.

[13] Engineering Toolbox. 2024. "Coefficients of Linear Thermal Expansion." https://www.engineeringtoolbox.com/linear-expansion-coefficients-d_95.html.

[14] Novozhilov, V. V. 1964. *Thin Shell Theory* (2nd ed.). Groningen: P. Noordhoff, Ltd.